Implementing Internal Heat Degradation Effects in Numerical Simulations of Miniature Circuit Breakers

Rodney Kleynhans, Jan-Hendrik Kruger, Pieter van Vuuren

***Abstract*—When a miniature circuit breaker (MCB) interrupts the flow of current due to a short circuit, it is a big event compared to the onload opening of contacts that causes internal damage to the MCB. Internal damage is not visible as a result of the construction of the MCB and is not easily measured while used. Thermal degradation is mainly due to the temperature of the arc and the time it takes to dissipate the arc when the contacts are opened. The erosion of the contact material is due to the heat flux of the arc during the opening, closing, or bouncing of contacts. This paper investigates the heat stress exerted on contacts during a short circuit and how that relates to the degradation of the contacts. Although the arc is short in duration, the energy is high at high temperatures. An Ansys model was developed to simulate how an MCB would radiate Joule heat based on default Ansys material property library values, and then after degradation has set in, by using experimentally measured values in the Ansys model. The Ansys simulations were verified through thermal images of an MCB internal conduction path that were subjected to a number of short circuits. The default library values had an over 26% discrepancy between the infrared (IR) and Ansys values. After adding the degradation calculation values to the Ansys simulation, the discrepancy decreased to 0.98%. The results clearly show that the material properties of the internal parts of the MCB changed during short circuits and affected the radiated heat measured with the thermal imager.**

***Index Terms*—Ansys, degradation, failure mechanisms, infrared, Joule heating, low-voltage, Maxwell, miniature circuit breaker, thermal imaging**

Open License: CC BY-NC-ND

I. Introduction

ELECTRICAL installation protection systems play a crucial role in the performance of equipment and the safety of personnel under abnormal conditions. Protection devices such as miniature circuit breakers (MCBs) are designed to detect electrical faults and quickly disconnect the fault component to reduce the effect of the fault on the rest of the installation. The speed at which the MCB disconnects the fault depends on the type of MCB and can be affected by temperature and other failure mechanisms, for example, fatigue failure. The importance of protection devices such as circuit breakers in a low-voltage (LV) network is often overlooked and can cause unnecessary damage to expensive equipment [1].

Rodney Kleynhans (corresponding author, e-mail: rodney@knt.co.za) and Prof. Pieter van Vuuren (e-mail: pieter.vanvuuren@nwu.ac.za) are with the School of Electrical, Electronic and Computer Engineering, North-West University, 11 Hoffman Street, Potchefstroom, 2531, South Africa.

Dr. Jan-Hendrik Kruger (e-mail: janhendrik.kruger@nwu.ac.za) is with the School of Mechanical Engineering, North-West University, 11 Hoffman Street, Potchefstroom, 2531, South Africa.

A. Degradation and failure mechanisms

The deterioration of electrical and mechanical equipment is unavoidable. Do we really understand the root of the degradation and what impact it has on the operation and remaining useful life (RUL) of the equipment? MCBs degrade daily while in use, and thermal degradation is accelerated by events such as continuous use at rated current (Joule heating), over current trips, and short-circuit trips. Processes that accelerate electrical degradation may include electrical heating, thermal degradation, and contact resistance [2].

Chen et al. [3] highlighted material transfer during the arcing process and concluded that material transfer is affected by material properties, electrical operation parameters, and surrounding gasses. IR experiments were restricted to the initiation and extinguishing of arcs, but not under fault conditions. Thermal arc plasma is a form of intense ultraviolet (UV) radiation and causes thermal degradation of the insulating materials and erosion of contacts, which directly affects the temperature distribution [4].

Therefore, it is expected that the duration and magnitude of the fault conditions will contribute to the overall degradation of the material and performance of a MCB. Degradation is a combination of various mechanisms such as physical (heat, force and radiation), chemical (oxidation and corrosion), and mechanical (frictural wear, fatigue, melting and fretting) and is summarized as in Table I. The effect of degradation can be measured either as changes in temperature and/or electrical resistance.

Borkowski [5] performed a comparative analysis of the heat transport pathways in switch gear considering general assumptions, initial conditions, and thermal models of the short arc between high-current contacts. The conclusion was that conduction is the dominant heat transfer mechanism, with convection and radiation inside a device having a negligible effect on the resulting temperature distribution.

To predict the lifetime of devices, we need to understand the dominant failure mechanisms. MCBs experience thermal, electrical, and mechanical stresses that gradually degrade the device leading to failure [6]. Covariates are factors that cause assets to degrade as they age or deteriorate and that impact the RUL. When a specified failure threshold is reached due to degradation, the assets fail. This may be forced, external to the system, or natural, age or time dependent. Degradation can be internal or external through environmental conditions.

Failures were categorized by [7] as:

TABLE I
SUMMARY OF DEGRADATION MECHANISMS

Mechanism of degradation	Degradation impacts the	Effects of degradation measured by change in
Current flow heat generation	Joule heating	Electrical resistance
Closing force between points	Arc conduction a-spots	Contact force Electrical resistance
Arc radiation heat generation	Arc conduction a-spots	Temperature
Chemical oxidation of points	Electrical conductivity	Temperature Electrical resistance
Corrosive wear of contact points	Material hardness Elec. conductivity	Temperature Electrical resistance
Adhesive wear	Material hardness Elec. conductivity	Temperature Electrical resistance
Abrasive and erosive wear	Material hardness Elec. conductivity	Temperature Electrical resistance
Mechanical fatigue	Material hardness Elec. conductivity	Temperature Electrical resistance
Contact arc melting of points	Material hardness Elec. conductivity	Temperature Electrical resistance
Contact arc fretting of points	Material hardness Elec. conductivity	Temperature Electrical resistance
Diffusive wear	Material hardness Elec. conductivity	Temperature Electrical resistance

- Soft failures or gradual failures that can be predicted by one or several condition monitoring indicators and are typically influenced by the age of the component or the history of the operating condition.
- The sudden or hard failure is a completely random failure and cannot be predicted by measuring the age of the asset alone.

B. Simulation of temperature distribution inside MCBs

Simulations of temperature distribution inside MCBs research focused on the details of the contact and arc regions and related heat transport or the changes related to material degradation. However, comprehensive and experimentally validated simulations that integrate these detailed effects to present a holistic thermal analysis of an MCB have been found to be lacking, especially when fault conditions were also considered.

Frei et al. developed a finite element model (FEM) that produced electrical (current density and voltage) and thermal (temperature and heat flux density) solutions [8]. Reports were generated for Joule heating, heat dissipation, locational temperatures, electrical voltage at these locations, electrical resistance of the individual parts, and electrical and thermal contact resistances. Although the results contribute to the study of the heat distribution inside a MCB, degradation and thermal stress caused by an arc were not considered. However, the material properties used in the simulation were theoretical values and were not obtained from measurements [8]. Shea simulated high-current arcs in the kA range and concluded that contact erosion was at its highest with a higher current density as the current increased and/or the contact area decreased [9]. Thangaraju et al. confirmed that FEM analyzes can be used to investigate Joule heating as a result of electrical resistance. The heat distribution was calculated from the current density and using a subroutine to input the heat flux from electrical calculations into the thermal heat analysis [10].

Huttner examined the thermal stresses along the current path through the contacts and found that the temperatures reach melting and evaporation limits. This illustrates the importance of knowing the temperature distribution, as it dictates the internal degradation of the MCB, with direct economic and reliability implications. Furthermore, Ansys simulations were used to calculate energy accumulation at contacts for various current amounts, but it was not confirmed by any experimental measurements [11]. Weibenfels et al. developed a theoretical 3D FEM model to investigate electrical conductance and electrical wear in electrical contacts. The heat dissipated by two contacts was shown to change with the force exerted on them, but no evidence was provided that the dissipation of the eroded contacts could be used as an indication of the degree of degradation [12].

Ren et al. [13] developed an FEM model of spherical copper contacts for a thermal-electrical analysis of Joule heating. The authors compared the simulation results with the calculation of the temperature-voltage equation to verify the Kohlrausch equation. Jiang et al. proposed a model to predict the endurance of electrical connectors considering the amplitude of microslip, contact force, overturning angle, superficial layer thickness, and frictional wear coefficients. Their theory of frictional energy dissipation is useful for analyzing contact failure due to wear [14]. Shen et al. developed a numerical approach to investigate the electrical-thermal-mechanical-wear coupling behavior of electrical contacts by means of an electrical contact conductance law together with the current conservation model. The effect of contact fretting influenced the electric potential and current density more than the temperature due to a decrease in resistance to electrical contact [15].

Although various studies considered heat transport inside MCBs due to specific but separated phenomena, there appears to be a lack of validated numerical analyzes of the internal temperature distribution as a result of the combined effects of Joule heating, eroding contacts, and varying material properties due to arc radiation. This contribution closes that gap by using experimentally measured material properties to incorporate degradation effects into numerical simulations, and subsequently validated that approach through thermal imaging of MCBs after various short circuits were applied.

The remainder of this paper is structured as follows. Background information on the construction and operation of MCBs is given in Section 2. Section 3 considers the heat distribution within an MCB. Section 4 describes the experimental methodology that was followed to obtain the properties of the material due to degradation, as well as its implementation in an Ansys FEM simulation. Section 5

summarizes the results, and Section 6 concludes.

II. Fundamental principals of an MCB

In this section, the construction, operation, and principal physics of MCBs are briefly described to give context to the modeling and experimental methodologies.

A. Construction and operation of an MCB

Without serviceable parts, the unit as a whole is replaced when it does not operate according to the manufacturer's chart. Low-voltage (LV) MCBs must be able to carry the rated current, interrupt an overload current, successfully interrupt short circuits, and enable manual on/off operations within the prescribed temperature and humidity ranges [1]. Successful current interruption occurs when the heat energy, due to the arc, inside the MCB is dissipated at the moment the contacts open [16].

The internal details of an MCB are shown in Fig. 1. There are five subsystems that work together to perform the functions mentioned above [1]. These subsystems are as follows:

1) Conduction path – Carries the rated current between the source and load terminals and consists of conducting elements and contact tips. Because the conduction path is the only heat source, it is primarily responsible for the increase in the temperature of the MCB.
2) Sensing unit - Detects current overload and initiates opening of the moving contacts. A hydraulic magnetic MCB operates by using the magnetic force produced by the current flowing through a coil where the coil and the load are in series. The coil is wound around a hermetically sealed tube that contains a mild steel core, a spring, and silicon oil as a hydraulic damping fluid. The magnetic flux created by the coil during an overcurrent event produces sufficient force to trip the mechanism.
3) Arc chamber - This is where the arc is formed during contact opening and is controlled and extinguished to interrupt the current. The purpose of arc grids is to split the arc into a number of shorter arcs and to cool the arc. Damage to the MCB is determined by the amount of energy that passes through and is determined by the opening time of the moving contacts and the efficiency of the magnetic force that blows the arc off the contact tips and into the arc grids.
4) Switch mechanism – Opens automatically when activated by the sensing unit, or opens and closes the moving contacts manually through the on/off handle. The speed depends on the type of MCB.
5) Moulded case – The housing of the MCB with sufficient structural integrity to withstand operating conditions and the required number of duty cycles.

B. Degradation mechanisms of contact points

The electrical contact points form the interface between the current-carrying members of electric devices to ensure the continuity of the electric circuit. The purpose of electrical contacts is to allow uninterrupted passage of electrical current through

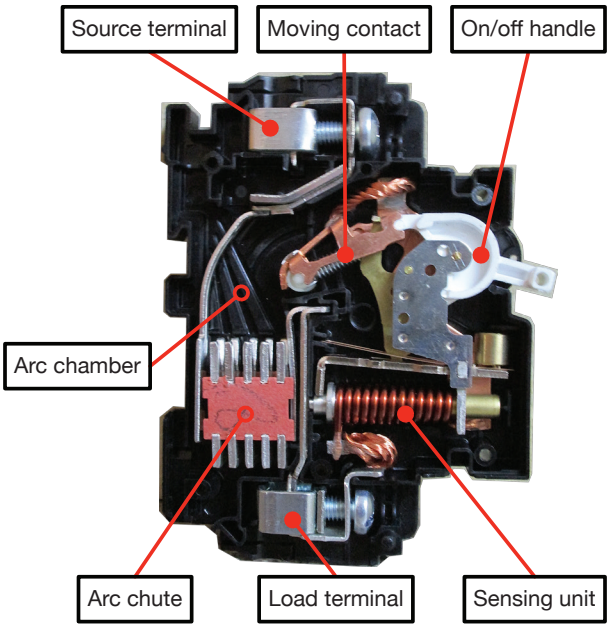

Fig. 1. Photograph showing the internal components, sub-systems and their configuration inside a typical MCB.

the electrical connection [17]. In miniature circuit breakers (MCBs), electrical contacts are essential components but are often taken for granted until they do not work as designed [18]. The solid surfaces of the contacts are not smooth but rough on a microscale. This roughness creates troughs and peaks that vary in shape, height, and other geometric characteristics. Due to the peaks and troughs, only a small fraction of the nominal contact area is the true area of contact. These mating areas are called a-spots. The reduced contact area at the a spots results in an increase in electrical resistance, also called interface constriction resistance [19].

Electrical contacts have the following requirements [17]:

Electrical: Low power losses, no signal distortion, and no overheating.

Mechanical: Stable contact force during closing and opening and high wear resistance.

According to Kesim et al. the most important degradation mechanism of contacts is arcing-induced erosion and oxidation accelerated by ozone (O_3) as a by-product of electrical arcs [20].

Because this mechanism affects the electrical and mechanical performance of contacts, a thorough understanding of the parameters affecting arc erosion is needed.

The degradation factors of MCBs that lead to possible failure usually manifest as the following:

Contact area: The A-spots create temperatures higher than normal as a result of increased resistance as a result of the constriction in the current flow area. A small drop in the contact voltage can substantially increase the temperature. This produces metallurgical changes, such as softening or even melting of the conducting areas. No deterioration is noticeable until failure and damage is cumulative. When local temperature increases, self-accelerated deterioration

is triggered by the interaction of thermal, chemical, mechanical, and electrical processes [17].

Oxidation: The loss of radical electrons through a chemical process that increases the oxygen content of a base metal is known as oxidation [17].

Corrosion: Corrosion causes the degradation of a metal component through chemical or electrochemical reactions with its surrounding environment. The most common types include atmospheric, localized, crevice, pitting, and galvanic corrosion [17].

C. Joule heat generation in contact points

The Joule heat generated in the contacts and other conductive elements depends on the electrical load and resistance. The heat source due to Joule heating (Q_{joule}) of the conduction path and contact resistance can be stated as [8]:

$$P = I^2 R_i \tag{1}$$

where I is the current carried in the specific conductive element and R_i the inherent resistance of the element under consideration.

The electrical resistance and heat generated tend to increase with age, caused by an agglomeration of mechanical and environmental factors. Therefore, the change in contact temperature over time can be used as a qualitative tool for the evaluation of contact conditions [21]. An increase in electrical resistance may be due to mechanical deterioration, corrosion, and / or contamination [22]. Chudnovsky et al. observed that a correlation between contact temperature measurement, ambient conditions, and load can identify abnormal physical conditions of contacts [22].

The inherent resistance R_i of the conduction path depends on the geometry and the specific electrical resistivity ρ_{el} of the material, as well as the length l and the cross-sectional area A:

$$R_i = \frac{\rho_{el} l}{A} \tag{2}$$

ρ_{el} is temperature dependent and is described by the temperature coefficient α_T [23]:

$$\rho_{el(T)} = \rho_{el(T_{20})} \cdot (1 + \alpha_T (T - T_{20})) \tag{3}$$

For this study, the value of electrical resistivity of copper α was acquired from [24] and that of silver from [25]. T is the temperature and T_{20} is the temperature at 20°C. The tests performed by Yu et al. revealed that the contact resistance of an untested MCB was low, with a low standard deviation and no oxidation. After overload testing, the contact resistance and standard deviation increased, including oxidation. Endurance testing revealed a contact resistance that was higher compared to that of untested MCBs, but lower than that of overload-tested MCBs. The standard deviation after the endurance test was much higher than after overload testing. This might be due to extensive erosion of the contact surface on one side and oxide buildup on the other side. The phenomena were due to the swiping motion of the contacts over each other during breaker closure. The highest contact resistance and standard deviation was observed after short circuit testing when much lower oxide levels were observed, but large midplane cracks developed due to thermal stress during the tests [26].

The contact temperature can be calculated by measuring the voltage drop across the closed contacts. Assuming that there is no radiated heat loss and that the equipotential lines are the same as the equitemperature line, the voltage drop V is given by:

$$V^2 = 8 \int_{T_0}^{T_P} \rho \lambda dT \tag{4}$$

where T_P is the maximum temperature the conductor reached, T_0 the ambient temperature, ρ the resistivity, and λ is the thermal conductivity [18].

The voltage drop can be rewritten in terms of the temperature differences by using the Wiedemann-Franz law.

$$\rho \lambda = L \theta \tag{5}$$

where θ represents the electrical conductivity of the material and L is the Lorenz constant given by:

$$L = \frac{\pi^2}{3} \left(\frac{k}{e} \right)^2 \tag{6}$$

with k being the Boltzmann constant, e is the electronic charge, and $L = 2.45 \times 10^{-8}\ W\Omega/\text{degree}^2$.

The reformulated expression for the voltage drop is then:

$$V = \left[4L \left(T_P^2 - T_0^2 \right) \right]^{1/2} \tag{7}$$

which can be simplified for large temperature differences, $T_P >> T_0$ to obtain:

$$T_P = \frac{V}{2\sqrt{L}} \tag{8}$$

D. AgMeO contact tips

Contact materials can be metal alloys, metal/oxide, or metal/refractory (M/R). M/R contacts have good electrical properties and high arc resistance. The metal component provides electrical and thermal conductivity while the refractory phase provides strength, welding, and erosion resistance. Silver is often used as a contact material as a result of its high thermal and electrical conductivity. The disadvantage of silver is that it has relatively low melting (961.8°C) and boiling points (2161°C), low mechanical strength, is prone to contact welding, and exhibits a tendency to form tarnishing films [20].

AgMeO (88/22) (Silver metal oxide) as a contact material has become very popular in switching devices due to its high resistance to erosion and contact welding. Silver has a high thermal and electrical conductivity. Metal oxide is used for its electrical properties and its high resistance to arcs. It also has a tendency to form sulfide films [27].

An arc inside an MCB can be as hot as 3700°C, and material transfer can take place between contacts. The arc has a high current density at the cathode and a low voltage drop at the cathode. Contact welding occurs when there is separation of

the silver and metal oxide components due to thermal stress. Ball-shaped silver beads accumulate on the surface, promoting contact welding. Moving contacts aggravate the problem and tend to lose more weight due to erosion when welded points break apart during operation. The separation of silver and metal oxide appears to be more distinctive in resistive loads than in inrush current loads. This is the result of a higher thermal stress [27].

With a short arc, contact separation between high current contacts, the thermal power received by the anode is 15% higher than that received by the cathode. The higher energy of the anode will result in more intense wear in the case of a short high-current arc [5].

When the contacts of AgMeO tips close, there is an anode mass loss and a cathode mass gain. This is due to an anodic arc caused by the gap between electrodes being shorter than the mean free path of the electrons. The electrons emitted from the cathode suffer minor collisions on their way to the anode and strike it with full energy. Due to electron bombardment, the anode evaporates and part of the resulting mass loss is collected by the cathode [28].

Therefore, arc erosion of the contact material through evaporation or molten liquid removal is one of the most important degradation mechanisms in mechanical switches. The physical characteristics of the arc column are fully described by considering the conservation laws of mass, momentum, and energy by including convective fluxes, conduction fluxes, radiation fluxes, and Joule heating [29], and serve to motivate the use of comprehensive simulation platforms (such as Ansys) when numerical analyzes are performed.

E. Electric arc energy

The electric arc that is formed when contacts separate inside an MCB under load is governed by the physics of electromagnetism and thermodynamics. The arc is highly resistive and generates a passive voltage that opposes the system voltage and brings the circuit current to zero [30]. The voltage of the arc is a function of the position of the moving contacts and is a function of the length of the arc [31]. The high-temperature plasma of the arc causes thermal degradation of the insulating materials and erosion of the contacts [4].

The energy of the arc (E_a) can be calculated with the following equation:

$$E_a = \int_0^t u_a(t) i(t) dt \tag{9}$$

where $u_a(t)$ is the voltage of the arc that changes with time, $i(t)$ is the current of the arc that changes with time [1].

F. Energy balance inside MCB and temperature distribution

Considering the complex combination of heat transfer modes inside an MCB, numerical solution methods are best suited for detailed analyzes. In this study, Ansys [32] was selected as the simulation framework, based on its ability to provide a multi-physics FEM framework in which electrical heat generation can be coupled to mechanical heat transfer effects and temperature distribution inside structural materials.

Conservation of energy, without mechanical work, dictates that conductive heat transfer (Q_c), convective heat transfer (Q_{cv}) and radiated heat transfer (Q_r) must be in balance with Joule heat generated [33]:

$$Q_r + Q_{cv} + Q_c = Q_{joule} \tag{10}$$

The heat required to change the temperature of a given component is proportional to the mass m of its material and the change in temperature ΔT [34]. The material is characterized by its specific heat capacity (c):

$$Q = mc\Delta T \tag{11}$$

The heat energy always flows from a hotter region to a colder region. The rate at which heat is conducted depends on the thermal conductivity k, the cross sectional area A of the object, the distance l between the ends and the temperature difference between the two ends ΔT, as stated in Eqn. (12) from [34]:

$$\frac{dQ}{dt} = kA\frac{\Delta T}{l} \tag{12}$$

The Stephan-Boltzmann formula is used to calculate the net flow rate of heat radiation between two bodies [34]. The rate at which a body radiates energy is proportional to the 4th power of its temperature:

$$\frac{dQ}{dt} = \varepsilon\sigma A(T_1^4 - T_2^4) \tag{13}$$

where ε is the emissivity (ability to radiate heat and is a factor between 0 and 1) and σ is the Stefan-Boltzmann constant with a value of $5.67 \times 10^{-8}\ W/m^2K^4$.

G. Electrical resistance as an indicator of condition

Changes in the geometric and material properties of the main contacts influence their electrical resistance [8]. Finding the electrical resistance of the main contacts starts with calculating the radius a_e of the elastically deformed contact area:

$$a_e = \sqrt[3]{\frac{3}{4}F_K\left(\frac{1-u_1^2}{E_1} + \frac{1-u_2^2}{E_2}\right)\left(\frac{1}{r_1} + \frac{1}{r_2}\right)^{-1}} \tag{14}$$

with F_K being the contact force, E the modulus of elasticity, u the Poisson's ratio and r the radii of the spherical members in contact.

With a_e known, the contact resistance R_E can be calculated from [8]:

$$R_E = \frac{\rho}{2a_e} \tag{15}$$

where ρ is the average specific electric resistivity of the two different materials in contact.

The electrical contact resistance R_{el} at the terminals can be calculated by:

$$R_{el} = \frac{C_\rho}{F_K^m} \tag{16}$$

where the product of C_ρ is a constant dependent on the materials in contact and m is an exponent dependent on the shape of the contacts [8].

TABLE II
TEMPERATURE-RISE LIMITS FOR TERMINALS AND ACCESSIBLE PARTS

Description of part	Temperature-rise limits (K)
Terminals for external connections	80
Manual operating means:	
metallic	25
non-metallic	35
Parts intended to be touched but not hand-held:	
metallic	40
non-metallic	50
Parts which need not be touched for normal operation:	
metallic	50
non-metallic	60

The electrical contact resistance R_{th} is derived from the thermal contact resistance:

$$R_{th} = \frac{R_{el}}{\rho\lambda} \tag{17}$$

with λ denoting the average thermal conductivity of two different materials in contact [8].

H. Condition assessment based on temperature

To assess the condition of the control and auxiliary circuits within an MCB, the increase in temperature during operation can be compared to the maximum allowable limits prescribed by industry standards, as the upper limit of an acceptable state. Table II from IEC 60947-2 [35] gives the allowable temperature increase limits for MCBs under rated operating conditions.

For electrical devices, temperature limits can therefore be determined from the rated ambient temperature limit, the allowable increase in temperature, and the maximum allowable operating temperature at the rated load and at a specified ambient temperature. In order to determine the maximum allowable temperature of a device at reduced load, the following formula is used:

$$T_{\text{maxcorr}} = \left(\frac{I_m}{I_z}\right)^2 T_{zw} + T_{0m} \tag{18}$$

where T_{maxcorr} is the corrected maximum allowable temperature, I_m is the measured load current, I_z the rated load current, T_{zw} is the rated rise in temperature and T_{0m} is the measured ambient temperature [36].

III. METHODOLOGY

Since an important aim of the current study was to obtain more realistic input values for simulations, to reflect the degradation of main contacts due to increased short-circuit activity, a three-step modeling strategy was developed. This strategy involved the development of a CAD model, the experimental measurement of the degraded electrical properties, and, lastly, their implementation in the simulations to validate the approach.

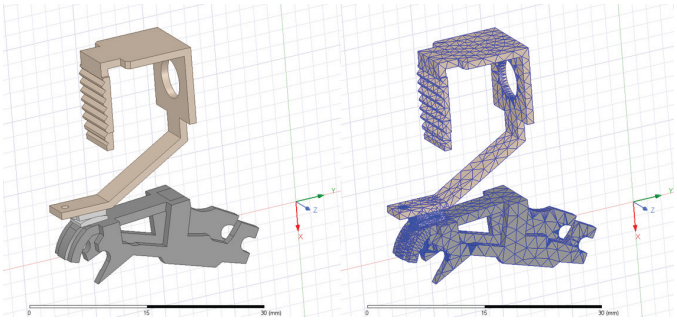

Fig. 2. Components of main current path constructed as CAD model and meshed inside Ansys.

A. Numerical simulation

Ansys [32] is a comprehensive multiphysics software suite used in the current study to simulate interactions between components by integrating electrical and thermal analysis. The core components of an MCB were simulated using an Ansys finite element model with sub-models for the combined effects of conduction, convection, and radiation. In order for the simulation tool to obtain realistic solutions, user inputs such as geometry, mesh, boundary conditions, and material properties were provided, in addition to the mathematical system that describes physics.

Through the incorporation of experimentally measured material property values from MCB short-circuit tests instead of the default Ansys library constants, it became possible to model changes in the temperature distribution as degradation sets in.

The following three steps comprise the simulation process:

1) Create CAD models of relevant components: The first step was to create a CAD model of the MCB terminal and contact region only and to import it into Ansys Maxwell 3D as the geometry to be simulated; see Fig. 2. Default mesh settings were found to be sufficient, as subsequent mesh refinement studies did not indicate a significant variance in the final results.

Ansys Maxwell 3D uses Finite Element Analysis (FEA) to simulate three-dimensional electromagnetic fields [32]. In terms of the solver type, DC conduction was selected because it has the ability to solve the electric field (E), current density (J), electric flux density (D) and DC current distribution. The current density results from the Maxwell simulation were then imported into Ansys Mechanical Desktop for thermal simulation to determine the temperature distribution (due to Joule heating) through the components.

2) Establish temperature-dependent resistance values: The second step was to determine the resistance values for components such as the source terminal, contact points, and the moving contact arm. These were calculated from the results of the RCL measurements of five MCB short circuit configurations, ranging from B0 (clean unused sample) to B4 (sample with four short circuits).

A Digimess 300 RCL meter was used to measure the values of R_i, and together with the length and area extracted from the CAD geometries, Eqn. (2) was used to calculate ρ_{el}.

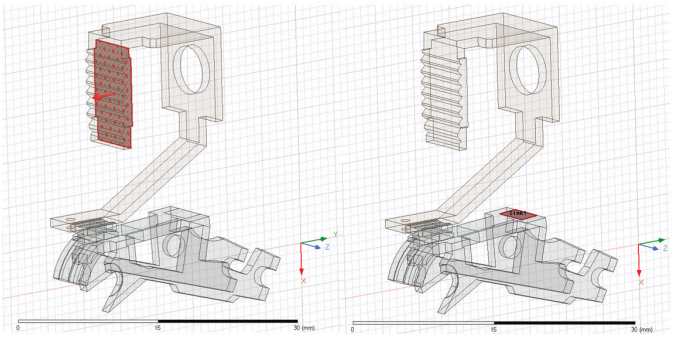

Fig. 3. Locations where the source excitations were applied to the numerical MCB model.

Eqn. (3) was used to calculate $\rho_{el(T)}$ at a specific temperature per component as measured with the thermal imager.

3) Apply custom resistance values in simulations: The third step involved the insertion of custom property values into the simulation workflow, where Ansys allows the user to adapt the built-in material properties to their own specialized requirements. In this case, the wear of the components was reflected in the changes in the bulk conductivity values, obtained from the inverse of the measured resistance ρ_{el}:

$$\text{Bulk conductivity} = \frac{1}{\rho_{el}} \tag{19}$$

The infrared temperature of the source terminal was used as the boundary temperature condition and the current as the input electrical condition, as shown in Fig. 3. The standard Mechanical Desktop solver was used with a convergence level of 30%.

B. Infrared measurements as validation

The calculated results from the Ansys model were verified by comparing them with physical measurements taken on MCBs subjected to various degrees of damage. For the practical experiment, a commercially available 20 A single pole curve 2 MCB was used and subjected to 3123 A short circuit test at ambient temperature, which aligns with the IEC 60947-2 international standard. The purpose of the short circuit test was to investigate its effects on internal degradation in the contact region after a number of short circuits and to determine whether the thermal imager's temperature values can be used as a measure of degradation.

The following steps were followed:

1) Apply short circuits: Four 20 A MCBs were subjected to 3123 A, 0.95 power factor, short circuits. In order to assess the degradation after each short circuit, the first MCB had one short circuit (B1), the second, two (B2), the third, three (B3) and the fourth, four (B4). The MCBs were then opened by removing the left shell to expose the internal parts. Because the internal parts are manufactured from copper, mild steel, and silver plated parts, the components were covered with a black high-emissivity paint to reduce reflectance for better temperature measurements with a thermal imager. The four test samples together with a clean (unused) control sample (B0) were connected in series to a DC power source to maintain constant current, to limit additional heat generation, due to the influence of alternating currents, such as eddy currents and core losses [23].

2) Heat up until steady state: The five MCBs were then allowed to heat up at 2 A load, for 30 minutes at ambient temperature, that is, until steady state was reached. Infrared thermal images of exposed internal MCB components were taken with a FLUKE Ti480 Pro radiometer (7.5 μm to 14 μm, ≤ 0.05°C at the target temperature of 30°C). Fluke SmartView software was used to measure the maximum temperature of each part individually.

During the experiment, ambient temperature and relative humidity were recorded with a Kestrel 3000 pocket weather meter. The voltage drop across the terminals was measured with a FLUKE 73 III multimeter to determine the combined resistance of the conduction path. The total resistance of the conduction path is the sum of the inherent resistances of the components, as well as the sum of the connection resistances. The thermal images as well as the resistance values obtained were used as reference values.

3) Repeat heating process with increased increments: Step 2 was repeated with the current increasing by 1 A increments until the rated current, 20 A, was reached.

Impedance measurements were taken with an automatic RCL meter of the source terminal, contacts, and moving contact arm of all sample MCBs, B0 to B4. This was used to calculate the resistances of the components of each of the five different MCB samples.

The Ansys model and the IR images showed changes in temperature in the contacts after each short circuit at the same current rating, 20 A. This implied a change in resistance according to the Joule heating formula:

$$P = I^2 R_i \tag{20}$$

where P is the power generated in the conducting material with inherent resistance R_i and subject to current flow of I.

IV. Results

A. Measured changes in resistance

The RCL measurements that were taken of the source terminals, contact points, and moving contact arms also revealed a change in the resistance of the source terminal and contacts, as shown in Fig. 4.

The change in resistance of the source terminals and contacts may be a result of a combination of the following effects:

- Carbon build-up on contacts,
- Slight changes in alignment of contacts due to movement,
- Contact erosion due to arc formation,
- A-spots leading to increased erosion,
- Contact force affecting the contact area,
- Softening of contacts, affecting contact area,
- Ozone (O_3) generated by the arcs that accelerates the corrosion of contacts, [20], and
- Degradation of the material by heat, leading to changes in properties.

Interestingly, the changes in resistance values of the moving contact arms were relatively insignificant, presumably because

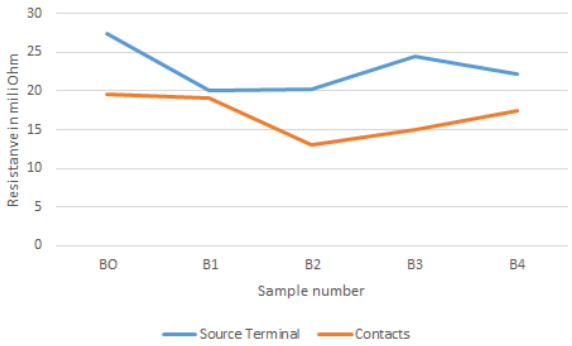

Fig. 4. B0 to B4 total resistance change as function of number of short circuits.

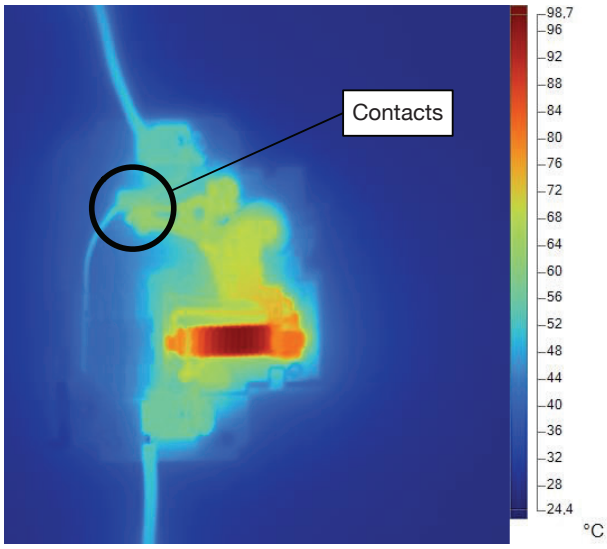

Fig. 5. B0 with no short circuits.

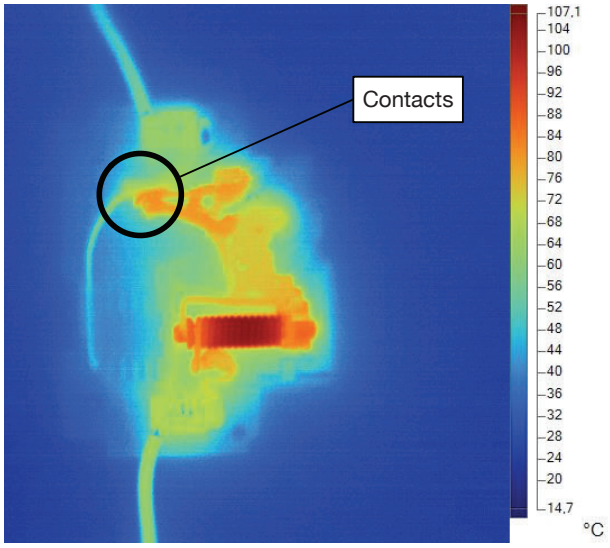

Fig. 6. B4 with four short circuits.

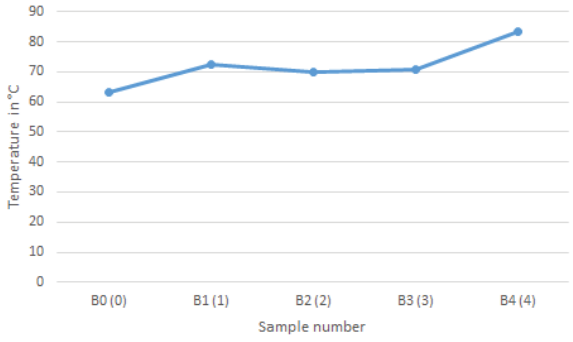

Fig. 7. Temperature increase of contacts at 20A after short circuits.

of the lower current density concentrations and nonexposure to arcs in that portion of the conduction pathway.

B. Infrared images of contacts

When comparing infrared images at 20A of the clean sample, Fig. 5, with the sample subjected to 4× short circuits, Fig. 6, a significant increase in temperature could be observed from 62.12°C to 83.19°C in the contact regions. These findings are represented in Fig. 7 and confirm that degradation has begun to set in and resulted in a resistance change that led to an increase in temperature. However, these values are still within the limits set by IEC 60947-2. During testing, the MCBs fail in the 5th short-circuit test.

C. Comparison between simulated and measured values

Table III is a summary of the IR and Ansys temperature values that highlights the difference when using the standard values from the Ansys library material and when using the measured degradation values of the different samples at 2 A, 10 A and 20 A. It is clear from the table that the library values alone are not sufficient for an accurate simulation. When the measured material properties were added to the Ansys simulation, the results could be validated with the values obtained by thermal imaging. A gradual increase in the difference between the IR temperature and the degradation temperature predicted by Ansys was observed from 10 A to 20 A for B0. This could be due to the influence of the materials that did not undergo a fault current.

Graphically, the comparison of Ansys simulation values with that of IR measurements for B0 and B4 can be summarized as seen in Fig. 8 and Fig. 9. B1, B2, and B3 had similar profiles.

V. Conclusion

When an MCB interrupts the flow of current due to a short circuit, it is a significant event that causes internal damage to the MCB. Material degradation is related to the temperature of the arc and how long it takes to extinguish the arc. That damage is not visible as a result of the construction of the MCB and is not easily measured while the MCB is installed and used. Thermal imaging, together with simulation, is therefore proposed as a non-invasive method to gage the level of deterioration inside an MCB.

The Ansys simulations employed in this study used a combination of calculations and measurements from MCBs

TABLE III
IR TEMPERATURE MEASUREMENTS FOR VARIOUS CURRENT LOADS, COMPARED WITH ANSYS SIMULATIONS WITH DEFAULT LIBRARY MATERIAL PROPERTIES, AND SIMULATIONS USING EXPERIMENTAL MEASUREMENTS OF DEGRADED PROPERTIES.

Sample	Current A	IR Temp °C	Library °C	Library % Diff	Degrad °C	Degrad % Diff
B0	2A	27.97	27.92	0.20%	27.96	0.04%
B1	2A	28.53	28.21	1.15%	28.23	1.06%
B2	2A	28.27	28.94	-2.30%	28.92	-2.25%
B3	2A	27.51	27.47	0.16%	27.47	0.13%
B4	2A	28.27	28.03	0.87%	28.04	0.81%
B0	10A	38.91	36.70	6.08%	41.17	-5.48%
B1	10A	43.06	38.84	10.91%	42.90	0.38%
B2	10A	40.97	38.41	6.66%	41.46	-1.18%
B3	10A	46.20	40.44	14.26%	44.10	4.77%
B4	10A	48.32	42.00	15.05%	45.97	5.12%
B0	20A	63.12	55.83	13.05%	75.68	-16.60%
B1	20A	72.47	59.78	21.22%	78.11	-7.22%
B2	20A	69.91	59.34	17.81%	73.16	-4.44%
B3	20A	70.89	57.02	24.32%	73.25	-3.22%
B4	20A	83.19	65.87	26.30%	84.01	-0.98%

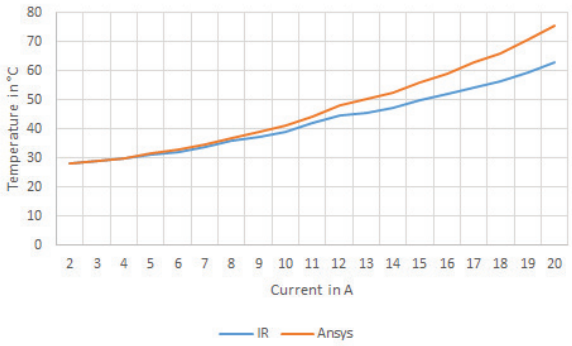

Fig. 8. B0 contact temperature as function of applied current.

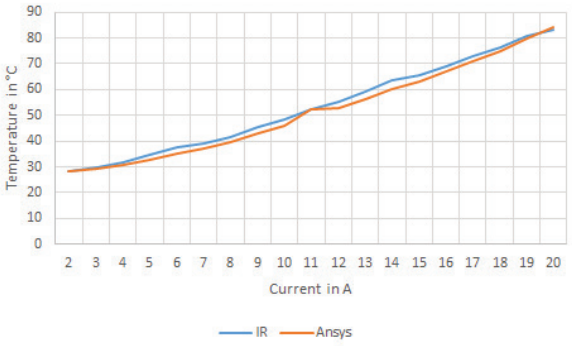

Fig. 9. B4 contact temperature as function of applied current.

subjected to short circuits, but focused only on the contact areas and main conduction path and did not include all of the individual parts that make up an MCB.

A simulation based on the default material properties found inside the Ansys library resulted in contact temperature values that significantly deviated from the IR measurements, more than 26%. With the experimentally measured material degradation values used in the simulation, the difference between IR and Ansys was reduced to less than 1% at 2 A and 20 A for sample B4.

The results confirmed that degradation did affect the Joule heating temperature of the MCB contacts and that the MCB simulations were valid only if degradation of the internal parts was taken into account through the use of material properties that were adjusted appropriately.

The next question is whether the heat of the internal conduction path of the MCB is conducted well enough to the outer shell so that the external temperature distribution can be evaluated to determine material damage. It is recommended that future research consider the link between the external and internal temperatures of MCBs before and after short circuits and to develop a health index (HI) that will assist in the prediction of remaining useful life (RUL) of MCBs.

REFERENCES

[1] Cohen Viv, *Application Guide for the Protection of L.V. Distribution Systems*. Creda Communications.
[2] Hattangadi AA, *Failure Prevention of Plant Machinery*. McGraw Hill Education Private Limited.
[3] Chen Zhuan-Ke and Sawa Koichiro, "Effect of arc behavior on material transfer: A review," vol. 21, no. 2, pp. 310–322.
[4] Thangarajan Beema R, Chetwani Satish, Shrinet Vagish, Oak Milind, and Jain Sachin, "A comparison of thermoset and thermoplastic arc chutes in molded-case circuit breakers under fault clearing," pp. 30–35.
[5] P. Borkowski and E. Walczuk, "Thermal models of short arc between high current contacts," pp. 259–264.
[6] Hanif Abu, Yu Yuechuan, DeVoto Douglas, and Khan Faisal, "A comprehensive review towards the state-of-the-art in failure and lifetime predictions of power electronic devices," vol. 34, no. 5, pp. 4729–4746.
[7] Gorjian Nima, Ma Lin, Mittinty Murthy, Yarlagadda Prasad, and Sun Yong, "A review on degradation models in reliability analysis."
[8] Frei Peter U and Weichert Hans O, "Advanced thermal simulation of a circuit breaker."
[9] Shea John J, "High current AC break arc contact erosion," in *Proceedings of the 54th IEEE Holm Conference*. Eaton Corporation.
[10] Thangaraju S M and Munisamy K M, "Electrical and joule heating relationship investigation using finete element method."
[11] Huttner L'udovit, "Thermal stress of contacts and current path of low-voltage switchgears," vol. 4, no. 4, pp. 32–36.
[12] WeiBenfels C and Wriggers P, "Numerical modeling of electrical contacts," vol. 46, pp. 301–314.
[13] Ren Wanbin, Wei Jianmin, Meng Xiangxing, and Zhi Hongxu, "Numerical simulation of temperature-voltage relation in electrical contacts and correction of classical khlrausch's equation," vol. 63, no. 3, pp. 1217–1224.
[14] Jiang Xiangjun, Pan Fengqun, Shao Guoqiang, Huang Jin, Hong Jun, and Zhou Aicheng, "Prediction of electrical contact endurance subject to micro-slip wear using friction energy dissipation approach," vol. 7, no. 6, pp. 537–550.
[15] Shen Fei and Ke Liao-Liang, "Numerical study of coupled electrical-thermal-mechanical-wear behavior in electrical contacts," vol. 11, no. 955.
[16] F. Bizzarri, A. M. Brambilla, L. Ghezzi, and F. Rigamonti, "Circuit level model of miniature circuit breakers," vol. 33, no. 6, pp. 2700–2709.
[17] Braunovic Milenko, Konchits Valery V, and Myshkin Nikolai K, *Fundamentals of Electrical Contacts*. Taylor & Francis Group.
[18] Browne Thomas E, *Circuit Interruption: Theory and Techniques*. Marcel Dekker.
[19] Slade Paul G, *Electrical Contacts: Principles and Applications*. Taylor & Francis Group.
[20] Kesim M T, Yu H, Aindow M, Alpay S P, and Sun, Y, "Corrosion, oxidation, erosion and performance of ag/w-based circuit breaker contacts: A review," vol. 12, no. 34.
[21] Livshitz Albert and Chudnovsky Bella H, "Condition diagnostics of energized electrical equipment: Case studies."

[22] Chudnovsky Bella H, Livshitz Albert, and Chudnovsky Borris A, "Thermal model of electrical contacts based on experimental data."
[23] Siegel Daniela and Anheuser Michael, "Significance of resistances of switching contacts for the temperature rise of LV circuit breakers."
[24] Matula R A, "Electrical resistivity of copper, gold, palladium, and silver," vol. 8, no. 4, p. 1147.
[25] Serway Raymond A, *Principles of Physics*. London: Saunders College Pub.
[26] Yu Haibo, Sun Yu, Kesim M Tumerkan, Harmon Jason, Potter Jonathan, Alpay S Pamir, and Aindow Mark, "Surface degradation of ag/w circuit breaker contacts during standardized UL testing," vol. 24, no. 9, pp. 3251–3262.
[27] Schoepf Thomas J and Hauner Franz, "Effects of different loads on the surface of silver metal oxide contacts for general-purpose relays," vol. 28, no. 4, pp. 728–733.
[28] Morin Laurent, Jemaa Nouredine Ben, and Jeannot Didier, "Make arc erosion and welding in the automotive area," vol. 23, no. 1, pp. 240–246.
[29] Swingler Jonathan and McBride John W, "Modeling of energy transport in arcing electrical contacts to determine mass loss," vol. 21, no. 1, pp. 30–54.
[30] Prabu Arulanantha, "An inverse problem approach to modeling of circuit breaker arc voltage."
[31] Stammberger Hartwig, Rümpler Christian, and Zacharias Albert, "Interactions in low–voltage switchgear-a staggered simulation approach."
[32] Ansys maxwell | electromechanical device analysis software. [Online]. Available: https://www.ansys.com/products/electronics/ansys-maxwell
[33] McIntosh Greg, "Surface temperature considerations."
[34] Giancoli Douglas C, *Physics: For Scientists & Engineers*. Prentice-Hall.
[35] "International standard IEC 60947-2." [Online]. Available: www.iec.ch
[36] Fidali Marek, "Thermographic criteria of evaluation of technical condition of machinery and equipment," vol. 61, no. 6, pp. 245–248.



Rodney Kleynhans received the degree Magister Technologiae electrical engineering from Central University of Technology, Bloemfontein, Free State, South Africa in 2012.

He is currently busy with his Ph.D. at North West University, South Africa. He is also a Level III ASNT certified thermographer with interests in electrical and mechanical hotspot detection. His research interest includes degradation and thermal pattern recognition.



Jan-Hendrik Kruger received the B.Eng. degree in mechanical engineering from the University of Pretoria, South Africa in 1997, an M.Eng. degree in mechanical engineering from the Potchefstroom University for CHE, South Africa in 2000 and the Ph.D. degree in mechanical engineering from North-West University, South Africa in 2005.

He is a senior lecturer in Fluid Mechanics at the School of Mechanical Engineering, North-West University (South Africa) with a keen interest in the practical use of engineering simulation across a wide range of applications. These include the use of computational fluid dynamics focussed on packed pebble bed thermal-hydraulics in nuclear reactors, centrifugal pump flow analysis, dilute phase gas-particle flow simulation, as well as aerodynamic analysis in the competitive sailplane and solar car racing environments.

Dr. Kruger has been an Executive committee member of South African Association for Theoretical and Applied Mechanics (SAAM) since 2018.



Pieter A. van Vuuren (M 2014) was born in Krugersdorp, South Africa in 1974. He received the Ph.D. degree in computer and electronic engineering from the North-West University in 2010. From 2010 to the present he has been part of the faculty of Engineering of the North-West University. His research interests include pattern recognition and machine learning applied to condition monitoring, agriculture and skills development.

CONTENTS PAGE